Determination of the discharge coefficient through vent driven by a non-Boussinesq plume in an emptying filling box

Yang Liu*, *Zhongwei* Huang, and *Lan* Huang

School of Civil and Surveying & Mapping Engineering, Jiangxi University of Science and Technology, Ganzhou, China

Abstract. The effect of high buoyancy forces due to density contrast between the fluids on either side of the vent on the discharge coefficient C_d is taken into account in the laboratory. Salt water experiments are conducted at small scale in a large fresh water tank with saline to generate buoyancy force. In non-Boussinesq cases, a larger discharge parameter Γ_d at the vent may make plume-like flow contract further with a smaller value of the discharge coefficient. A nearly twofold time in the non-dimensional form for draining light fluid fully out of the space is observed comparing with time predicted with a constant value of $C_d = 0.6$ for simple draining flows. A displacement flow theoretical model with virtual source correction at the initial position of an internal source is developed to reveal a time-dependent movement of the layer interface, and the oscillatory amplitude of the interface overshooting during the transient period is found to depend on the two dimensionless geometrical parameters Λ and Θ.

1 Introduction

Natural ventilation has become an important and attractive way to provide a comfortable indoor environment for potential savings in increasing energy costs[1]. A deeper understanding to ventilation is necessary for designing and operating ventilation systems more efficiently. Many heat sources in buildings can be regarded as localized ones which may be modeled by ideal plumes in a laboratory. Based on the classical plume theory developed by Morton, Taylor and Turner[2] (MTT), Baines and Turner[3] analyzed the effect of a buoyant plume on the properties of a uniform environment in a confined space which is attributed as the 'filling box' model. Linden et al.[4] extended the filling box model by placing vents on the emptying-filling box and studied the effect of internal sources on displacement and mixing flows.

The emptying-filling model studied by Linden et al.[4] revealed a major result that the buoyant layer thickness at steady state is independent of the strength of the source but a function of the vent areas, the height of the space, and the discharge coefficient C_d besides the entrainment coefficient of a Boussinesq plume. The discharge coefficient C_d is the ratio of the real flow rate to the idealized flow rate predicted by inviscid flow theory. Over a wide range in area ratios, C_d is taken as a constant of 0.6 for flow through openings in building. However, some measurements[5,6] in a laboratory indicate discharge coefficient to vary between 0.55 and 1 depending on opening type, vent area and temperature variation. Considering the effect of buoyant force in the field of building ventilation, C_d was firstly deduced from two series experiments of fluid draining and steady flow by Hunt and Holford[7,8] and was found to exhibit obvious dependence on density contrast in Boussinesq cases. The density contrast is embodied in the discharge parameter Γ_d which can be quantified with the ratio of buoyancy to momentum of the plume-like flow above the vent. In a recent paper, Mehaddi et al.[9] studied the dynamics of emptying-filling model driven by negatively buoyant and positively buoyant discharges with non assumption about the magnitude of the density deficit. However, the dependence of C_d on high density contrast in a non-Boussinesq case is not given definitely so far. Vauquelin et al.[10] also theoretically analyzed the dynamical displacement flow in the emptying-filling model within the non-Boussinesq limit. However, the overshooting behaviour of buoyant layer interface was illustrated according to the experimental results from Holford and Hunt[8].

The objective of this paper is to extend the experiments conducted by Hunt and Holford[7,8] for measuring the discharge coefficient C_d to non-Boussinesq circumstances. The time-dependent displacement flow activated by an internal heat plume is also investigated in the emptying-filling space.

2 The emptying filling box model with a non-Boussinesq plume

As shown in Fig. 1, an internal (non-Boussinesq) plume of buoyancy flux B is rising from an area source in a cubic box of height H and horizontal area S. An upper vent of area A is located at the ceiling of the box and a large lower vent at the floor. The buoyant fluid entrained by the

* Corresponding author: jxlgliuyang@163.com

turbulent plume is accumulated in the upper part, and then will drive a flow through the vents for the hydrostatic pressure difference between the lighter fluid in the box and the denser fluid outside the space. Thus, a buoyant layer of density ρ_b and thickness h will form beneath the ceiling and the buoyant fluid escapes through the vent at the top of the box with a mean velocity w. After the interface between ambient fluid and buoyant fluid descents from the initial time t=0, an ideal displacement flow forms.

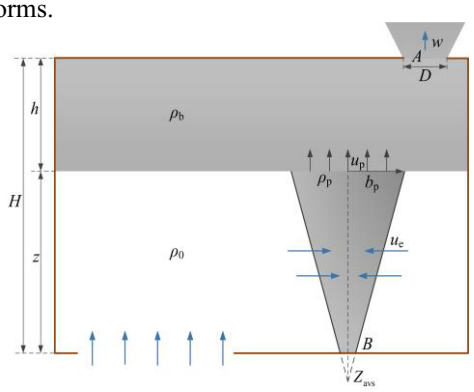

Fig. 1. Schematic diagram of steady displacement flow with an internal source of buoyancy.

For an axisymmetric plume, the description of a plume can often be simplified by taking the plume radius b, average values of the vertical velocity u and the reduced gravity g' in the cross section of the plume[11]. In terms of the top-hat variables, the equations of volume flux, momentum flux and buoyancy flux have been obtained by integrating across the turbulent plume. Rooney and Linden[12] (RL) extend the plume analysis of MTT model to the non-Boussinesq plume rising from a point source. The group solutions in a similarity form of these equations are given by Carlotti and Hunt[13] for a non-Boussinesq plume:

$$u = (3/4)^{1/3}(6\alpha/5)^{-2/3}\pi^{-1/3}B^{1/3}z^{-1/3}, \quad (1)$$

$$b = \frac{6}{5}\alpha(\rho/\rho_0)^{-1/2}z, \quad (2)$$

$$g(\rho-\rho_0)/\rho = -(4/3)^{1/3}(6\alpha/5)^{-4/3}\pi^{-2/3}B^{2/3}z^{-5/3}. \quad (3)$$

where u denotes the plume velocity, ρ and ρ_0 denote the density of the plume and the ambient respectively, and B denotes the buoyancy flux of the plume.

The conservation equations of the mass and the buoyancy flux are, for the buoyant layer, respectively:

$$\frac{d\rho_b Sh}{dt} = \rho_p \pi b_p^2 u_p - \rho_b wA, \quad (4)$$

$$\frac{d}{dt}\left[g\frac{\Delta\rho}{\rho_0}Sh\right] = B - g\frac{\Delta\rho}{\rho_0}wA, \quad (5)$$

where $\Delta\rho = \rho_0 - \rho_b$ denotes the density deficit of the buoyant layer.

Before proceeding the conservation equations, Bernoulli's theorem between the interface and the vent must be applied to evaluate the exit velocity $w=C_d\sqrt{2\frac{\Delta\rho}{\rho}gh}$. Following the definition from Vauquelin[10], the dimensionless variable $\zeta = z/H$, $\eta = \Delta\rho/\rho_b$ and $\omega = w/\sqrt{gH}$ are introduced and then Eqs.(4)-(5) and ω are rewrited as

$$\frac{d\zeta}{d\tau} = \Lambda\omega - k\Theta^{1/2}\left(\zeta^{5/3}+\Theta\right), \quad (6)$$

$$\frac{d\eta}{d\tau} = \frac{1+\eta}{1-\zeta}k\Theta^{1/2}\left(\Theta-\eta\zeta^{5/3}\right), \quad (7)$$

$$\omega = C_d\sqrt{2\eta(1-\zeta)}, \quad (8)$$

with $k = 18\sqrt{3}\alpha^2\pi/25$ and $\Theta = 4E^{2/3}B^{2/3}/3gH^{5/3}$ where Λ denotes a geometrical ratio of A to H^2, τ denotes the dimensionless time equal to $g^{1/2}H^{3/2}t/S$ and E is a constant equal to $25/48\pi\alpha^2$.

For a salt solution is released from a nozzle with a finite area source in the experiments, the vertical height of the interface can be corrected using a virtual origin height z_{avs}[14]. So z and H in Fig. 1 should be replace by $z+z_{avs}$ and $H+z_{avs}$, separately.

3 Experimental method

Fresh water and salt solution were used to create density difference in a large Plexiglas tank, and the stack-driven flow was in a direction contrast to that observed upward in building spaces. The schematic of the experiment set-up including a saline supply tank and an image processing unit is shown in Fig. 2.

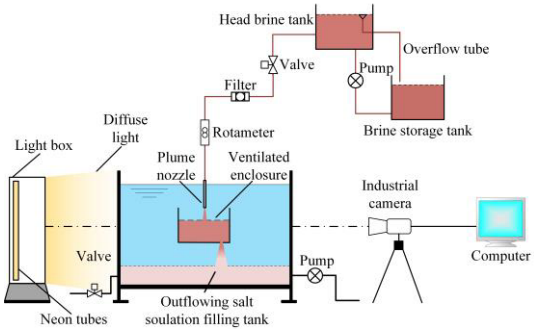

Fig. 2. Schematic diagram of the experimental apparatus using saline solution

Two series of experiments were conducted in the laboratory. In the first series, the discharge characters of the lower vent were examined as a buoyant fluid drained from a space in the displacement mode. In the second series, a steady stratification was established by releasing a buoyant source in a container and the corresponding discharge coefficient was deduced.

4 Results and discussion

The discharge coefficient C_d associated with the dense fluid through the circular vent is inferred from the measurement results, which as function of Γ_d is illustrated in Fig. 3. Γ_d is called the plume parameter in this context[10], and it is expressed as $\Gamma_d = 5(\rho_0 - \rho)gb/8\alpha\rho^{1/2}\rho_0^{1/2}u^2$. Triangle symbol presents experimental data from transient state in the first series, while square symbol indicates that from steady state in the second series. A least square fit to these discrete points yields the empirical formula:

$$C_d = 0.028 + 2.39(\Gamma_d + 12.48)^{-0.552}. \quad (9)$$

The empirical fit marked as the thick solid curve in the figure follows the same trend of experimental data from transient emptying and steady displacement. In the absence of buoyant flux, i.e. Γ_d=0, the curve suggests C_d=0.621, which is consistent with the value often used in calculation of flow rate through a sharp-edged opening[15]. The discharge coefficient descends to 0.2 approximately at the discharge parameter value of 100, and then goes on to fell at relatively slower rate towards 0.028. Distinguished from the illustration on the half log plot in the figure, actually the second derivative of C_d monotonously approaches zero with increasing Γ_d in the ordinary Cartesion coordinates.

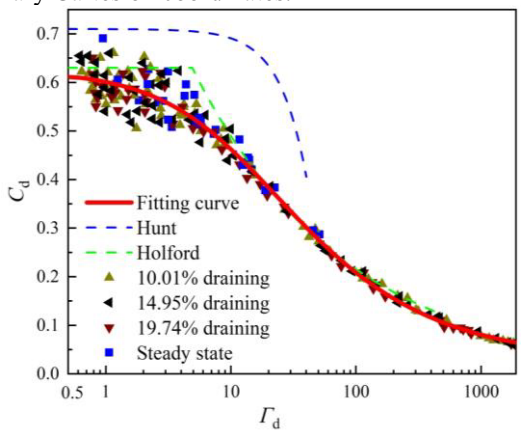

Fig. 3. Discharge coefficient C_d as a function of the discharge parameter Γ_d

For draining flows, it is supposed that heavy fluid of uniform density is fully filled in a container with one vent of area a_1 in the floor and one vent of area a_2 in the ceiling. As shown in Fig. 4, constant H is the height of the ceiling from the bottom, S is the cross-section area of the horizontal surface, and u_1 and u_2 are the velocity of the fluid through the lower and upper openings, separately. It is reasonable to assume that the incoming environmental fluid does not mix with buoyant layer but forms an ambient fluid layer which increases in height h with stack-driven fluid gradually draining from the vent in the floor.

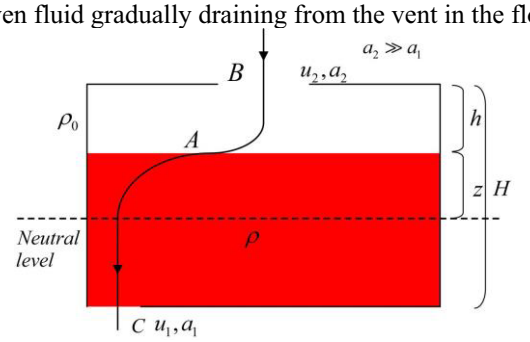

Fig. 4. Displacement flow from a container containing fluid of uniform density

In this emptying box problem, the flow at the lower vent is characterized by its velocity w, its density deficit η and its equivalent radius which can be expressed as $\sqrt{a_1/\pi}$ with a_1 the vent area. The plume parameter Γ_d of the plume-like flow that descends from the vent then reads

$$\Gamma_d = \frac{5}{16\alpha}\frac{1}{C_d^2}\frac{\sqrt{\Lambda/\pi}}{(1-\hat{h})\sqrt{1+\eta}}. \quad (10)$$

with $\Lambda = a_1/H^2$.

The dimensionless interface height from laboratory measurement is plotted as a function of the dimensionless time in Fig. 5 along with the theoretical predictions. At the first stage the interface quickly arrives about 95% of the rectangular height in nearly half emptying time, and then, it needs another half time for dense fluid of left 5% volume to drain out of the container at the second stage. The discharge coefficient deduced from the experimental measurement decreases relatively slowly at the initial moment of emptying flow. And then C_d drops significantly during the transient period between the two stages before finally approaches the constant value.

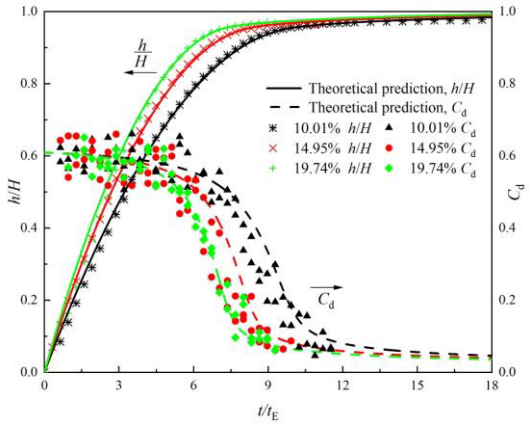

Fig. 5. Time evolutions of the dimensionless interface heights of displacement flow with various densities of salt solution

In the second series of experiments, displacement flows were established by locating a buoyancy point source on the top of the container, positioned at a wide range of heights from 15.7 to 32.0 cm above the base. Fig. 6 demonstrates the evolution of the dimensionless interface height ζ as a function of the non-dimensional time τ. It is obvious that the interface height overshooting happens when comparing with the final steady position for various nozzle positions.

After simultaneous emptying and filling flows begin, the buoyant layer is supplied with a volume flux by the plume through the interface and hydrostatic pressure difference produced by buoyant fluid drives the volume flux out of the upper opening. When the interface descending towards the plume initially approaches the equilibrium position at the steady state, the mass flow rate out of the opening is less than that supplied by the plume for the change in the discharge coefficient C_d through upper opening lag behind the thickness change in the buoyant layer. As a result, the height of the interface would go on downwards to overshoot beyond the equilibrium position until the mass flow rate draining at the top vent balances the mass flow rate of the plume through the interface.

In a similar way, an upward overshooting could be explained by the fact that the mass flow rate out of the container is larger than that flowing into the buoyant layer when the interface reaches the steady state position at the second time since the bigger discharge coefficient at this moment is leaded to by the thicker buoyant layer before. The process will continue and the interface oscillates around at the equilibrium height until the final steady state is arrived.

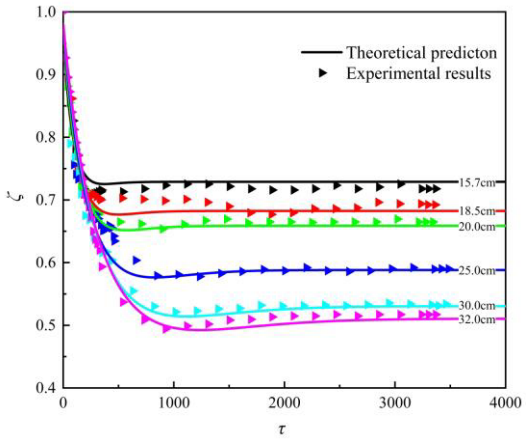

Fig. 6. Evolution and overshoot of ζ as a function of τ with various nozzle positions

Also shown in Fig. 6 are the theoretical curves for the dimensionless interface heights plotted against the non-dimensional time. There is good quantitative agreement with the experimental results with various nozzle positions generally. The collapse of the data at the initial period with the two-fold variation in the nozzle height supports the assumption that negligible overturning is reasonable to the outflow from the plume in the enclosure for aspect ratio of H/R=1.50. Subsequently, the theoretical curves match the experimental results quite well until the interface reaches its steady state height. It is clearly illustrated in the figure that the vibration of interface is intensified and the interface need more time to approach the minimum height with increasing nozzle height from 15.7 to 32.0 cm. During this process, the dimensionless interface height at the steady state decreases from 0.7288 to 0.5102.

5 Conclusions

In the presence of large density contrast, the discharge coefficient C_d through a horizontal opening is deduced from interface measurement of a stratification fluid produced by both an internal plume source and dense salt solution in an emptying-filling box. The density contrast is embodied in the discharge parameter Γ_d at the opening which reflects the relative importance of buoyant force and inertial force. Discharge fluid from a large opening with high buoyancy and low velocity gives obvious contraction and a large value of Γ_d with a small value of the discharge coefficient. The experiments of displacement flow are conducted as a fluid with different density from the environment is initially filling in an envelope with upper and lower openings. In the non-Boussinesq case, theoretical analysis for draining the dense fluid fully out of the container displays a nearly twofold magnitude in dimensionless time using a changed discharge coefficient comparing with that predicted with a constant value. The overshooting is observed for the buoyant layer depth descending below the steady-state depth and oscillates asymptotically to the final value. A theoretical model with virtual source correction below the actual position is developed to exhibit a time-dependent movement of the buoyant layer interface.

Acknowledgements

This research is supported by the National Natural Science Foundation of China (No. 52068031), Natural Science Foundation of Jiangxi Province of China (No. 20202BABL204062).

References

[1] T. D. Higton, H. C. Burridge, G. O. Hughes, Build Environ, **203**, 108093 (2021)
[2] B. R. Morton, G. Taylor, J. S. Turner, P. Roy. Soc. Lond., **234**, 1-23 (1956)
[3] W. D. Baines, J. S. Turner, J. Fluid Mech., **37**, 51-80 (1969)
[4] P. F. Linden, G. F. Lane-Serff, D. A. Smeed, J. Fluid Mech., **212**, 309-335 (1990)
[5] C. R. Chu, Y. H. Chiu, Y. W. Wang, Energy Build., **42**, 667-673 (2010)
[6] Q. H. Liao, Y. L. Guan, Q. N. Wang, Appl. Mech. Mater., **525**, 420-426 (2014)
[7] G. R. Hunt, J. M. Holford. *The discharge coefficient–experimental measurement of a dependence on density contrast*, in Proceedings of 21st International AIVC Conference, 12-24 (2000)
[8] J. M. Holford, G. R. Hunt. *The dependence of the discharge coefficient on density contrast–experimental measurements*, in Proceedings 14th Australasian Fluid Mechanics Conference, 123-126 (2001)
[9] R. Mehaddi, P. Boulet, M. Koutaiba, et al., Phys. Rev. Fluid, **6**, 083801 (2021)
[10] O. Vauquelin, E. M. Koutaiba, E. Blanchard, et al., J. Fluid Mech., **817**, 171-182 (2017)
[11] J. S. Turner, Buoyancy Effects in Fluids (Cambridge University Press, Cambridge, 1973)
[12] G. Rooney, P. Linden, J. Fluid Mech., **318**, 237-250 (1996)
[13] P. Carlotti, G. R. Hunt, J. Fluid Mech., **538**, 343-359 (2005)
[14] T. S. Van Den Bremer, G. R. Hunt, J. Fluid Mech., **644**, 165-192 (2010)
[15] D. W. Etheridge, M. Sandberg, Building ventilation: theory and measurement, **50** (John Wiley & Sons Chichester, UK, 1996)